Received: 5 June 2024 | Revised: 2 April 2025 | Accepted: 21 April 2025

DOI: 10.1002/pro.70153

RESEARCH ARTICLE

THE PROTEIN SOCIETY WILEY

Molecular characterization of a synthetic neutralizing antibody targeting p67 of *Theileria parva*

Shane Miersch[1] | **Alex U. Singer**[1] | **Chao Chen**[2] | **Fred Fellouse**[3] | **Anupriya Gopalsamy**[1] | **Luciano Silva e Costa**[1] | **Anna Lacasta**[4] | **Hannah Chege**[4] | **Naomi Chege**[4] | **Vishvanath Nene**[4] | **Sachdev S. Sidhu**[1]

[1]The School of Pharmacy, University of Waterloo, Waterloo, Ontario, Canada

[2]The Hospital for Sick Children Research Institute, University of Toronto, Toronto, Ontario, Canada

[3]Research and Development, Abtech Therapeutics, Marseille, France

[4]Animal and Human Health Program, International Livestock Research Institute, Nairobi, Kenya

Correspondence
Vishvanath Nene, Animal and Human Health Program, International Livestock Research Institute, Nairobi, 00100, Kenya.
Email: v.nene@cgiar.org

Sachdev S. Sidhu, The School of Pharmacy, University of Waterloo, Waterloo, Ontario, N2L 3G, Canada.
Email: sachdev.sidhu@uwaterloo.ca

Review Editor: Aitziber L. Cortajarena

Abstract

The *Theileria parva* sporozoite surface antigen p67 is a target of the bovine humoral immune response that generates antibodies capable of providing protection against subsequent infection. As a result, p67 has been the subject of efforts aimed at the development of an anti-sporozoite subunit vaccine. Previous studies have identified neutralizing epitopes in the N- and C-terminal regions of the full-length protein and shown that immunization with a C-terminal fragment of p67 (p67C) alone is capable of eliciting protection. To identify additional neutralizing epitopes in p67C, selections were conducted against it using a phage-displayed synthetic antibody library. An antibody that neutralized the sporozoite in vitro was identified, and the crystal structure of a Fab:peptide complex was elucidated. Mutagenesis studies aimed at validating and further characterizing the Fab:peptide interaction identified critical residues involved in binding and neutralization. This study also validates distinct epitopes for previously reported neutralizing antibodies.

KEYWORDS

crystal structure, neutralizing, p67, parasite, synthetic antibody, *Theileria parva*

1 | INTRODUCTION

Theileria parva, the causative agent of East Coast fever (ECF), is a tick-transmitted intracellular protozoan parasite that infects cattle and causes an acute lymphoproliferative infection, which is often lethal and exacts substantial economic losses in countries in sub-Saharan Africa (Nene & Morrison, 2016; Norval et al., 1992). Disease control measures are exacerbated by the presence of an asymptomatic wildlife reservoir of *T. parva* in African buffalo, although in cattle, buffalo-type parasites present a different clinical condition called corridor disease. Though several conventional methods (e.g., acaricides and chemotherapy) can be used to control disease (Norval et al., 1992), development of resistance, high costs, and inefficiency of treatment preclude widespread access for many farmers. An efficacious live-sporozoite-based infection and treatment method (ITM) of immunization is available, but it has been difficult to manufacture and deliver this vaccine in a sustainable manner (Gharbi & Darghouth, 2015; Perry, 2016; Radley et al., 1975). As a result, efforts are ongoing to develop a cost-effective, subunit vaccine that provides broad protection against the diversity of circulating *T. parva* strains (Nene & Morrison, 2016).

Inoculation of immune cattle with cryopreserved *T. parva* sporozoites elicits antibodies that can neutralize infectivity (Radley et al., 1975) by primarily targeting a sporozoite surface antigen that is highly conserved among cattle-isolated strains (Musoke et al., 1984; Nene et al., 1996). The discovery of a common

protective antigenic determinant led to the identification of the surface antigen as the protein p67 (Nene et al., 1992). Studies using recombinant, full-length p67 as an immunogen elicited immunity to sporozoite challenge (Bishop et al., 2003; Musoke et al., 1992; Musoke et al., 2005). Based on these observations, and the fact that isolated full-length protein can competitively inhibit parasite entry (Shaw et al., 1995), p67 has been attributed a putative role in host cell recognition and entry to facilitate the infection of bovine T and B cells. However, the production of full-length p67 protein for use as a vaccine remains a technical challenge, as yields are unsuitable for widespread and cost-effective prophylactic applications (Tebaldi et al., 2017).

Efforts to define epitopes on p67 that could form the basis of a subunit vaccine revealed that sporozoite-neutralizing, polyclonal antibodies—obtained by bovine immunization with full-length p67—target regions in the N- and C-terminal regions of p67 (Bishop et al., 2003; Nene et al., 1999), suggesting the importance of these regions in infectivity and immunity. Similar efforts identified murine monoclonal antibodies (mAbs) AR22.7 and AR21.4, which target discrete linear B cell epitopes in the N- or C-terminal regions, respectively (Nene et al., 1999). In fact, it was shown that levels of protection equivalent to immunization with a near-full-length recombinant version of p67 could be achieved by immunization with an 80-residue C-terminal peptide referred to as p67C (residues 572–651) (Bishop et al., 2003; Musoke et al., 2005). However, repeated inoculations with high doses of p67C were required to achieve immunity, thus precluding its widespread use as a subunit vaccine. Consequently, efforts to identify suitable p67 subunits and additional sporozoite antigens (Nyagwange et al., 2018) for use as vaccines are ongoing (Lacasta et al., 2018a; Lacasta et al., 2021a; Lacasta et al., 2023; Nene & Morrison, 2016).

To determine whether p67C contains additional neutralizing epitopes, we screened a phage-displayed, antigen-binding fragment (Fab) library (Persson et al., 2013) and identified an antibody (B11) that neutralizes sporozoite in vitro and targets an epitope distinct from those previously reported. Structural characterization of the Fab-B11:p67C complex by x-ray crystallography revealed that the antibody recognizes a 20-residue polypeptide consisting of a helix preceded by an N-terminal strand. To validate the structure and determine critical binding residues, we used a series of alanine-scanning variants of the 20-residue polypeptide to evaluate interactions with Fab B11 by biolayer interferometry (BLI). In parallel, we also validated and compared the potency of B11 antibodies to another sporozoite-neutralizing monoclonal antibody (AR21.4) reported to target linear epitopes within p67C (Nene et al., 1999). Chimeric human IgG1 versions of these murine antibodies were produced and specificities for their putative peptide epitopes were confirmed. Overall, our study provides details of epitopes within p67 that can be targeted by antibodies for neutralization of *T. parva* infectivity and validates recombinant tools that will facilitate future inquiry into p67-directed, protective immune responses against ECF in cattle.

2 | RESULTS

2.1 | A phage-derived synthetic Fab binds specifically to p67

Given the ability of immunization with p67C to induce immunity to ECF (Bishop et al., 2003; Musoke et al., 2005; Nene et al., 1999), we sought to identify neutralizing epitopes within p67C by conducting selections using a phage-displayed, synthetic human Fab library (Persson et al., 2013). Following four rounds of selection against immobilized GST-p67C fusion protein, 96 individual clones were isolated and evaluated for binding to p67C by phage ELISA. This analysis identified 26 clones that bound specifically to p67C and not to the fusion tag, and DNA sequencing showed that these clones all represented a single unique antibody, which we named B11 (Figure 1a).

2.2 | Fab B11 binds full-length p67 and an epitope in p67C

Binding of a range of concentrations of Fab B11 to full-length p67 was verified by BLI, enabling determination of a K_D value of 79 nM (Figure 1b). To evaluate the binding and specificity of Fab B11 by ELISA, serial dilutions of Fab protein were exposed to immobilized His-p67C and negative control proteins (ubiquitin and bovine serum albumin). Fab binding signals obtained following development with an HRP-fused anti-kappa secondary IgG revealed dose-dependent binding to p67C with an EC_{50} of 25 nM and no detectable binding to either control protein (Figure 1c). We also used ELISAs to compare Fab B11 with chimeric IgGs AR21.4 and AR22.7. All three antibodies bound to full-length p67, and as expected, IgG AR22.7 bound to p67N, whereas IgG AR21.4 and Fab B11 bound to p67C (Figure 1d). We further dissected the epitopes of Fab B11 and IgG AR21.4 by ELISA with two fragments of p67C named $p67^1$ (Nene & Morrison, 2016) (residues 572–612) and $p67^2$ (Norval et al., 1992) (residues 613–651). These assays showed that Fab B11 bound to $p67^1$, whereas IgG AR21.4 bound to $p67^2$ (Figure 1e), and non-overlapping epitopes were further confirmed by the fact that both antibodies could bind simultaneously to p67C (data not shown).

2.3 | p67-binding antibodies neutralize sporozoites in vitro

Fab B11 was evaluated in parallel with its IgG1 analog (IgG B11) and the chimeric IgG 21.4 (described in

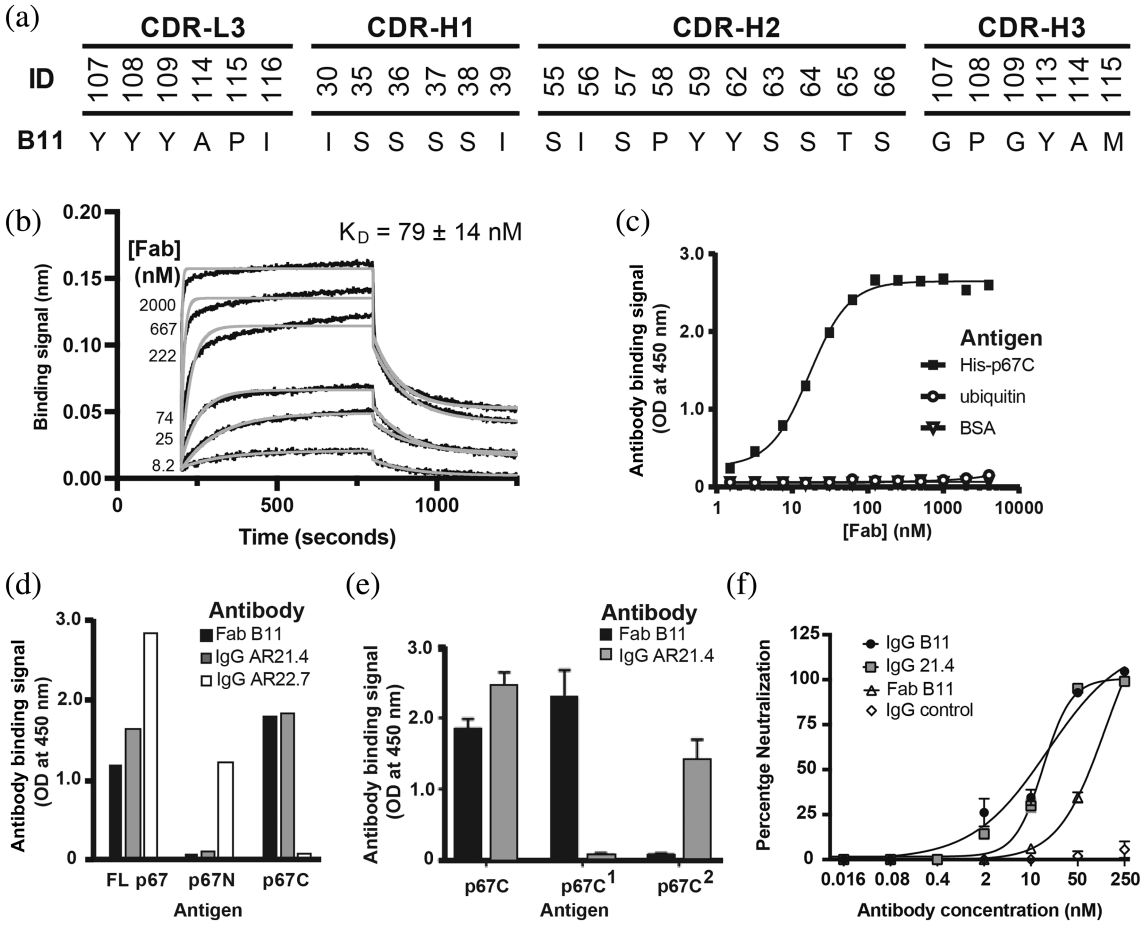

FIGURE 1 Characterization of Fab B11. (a) Sequences of Fab B11 CDRs. Only positions that were diversified in the phage-displayed library are shown and are numbered according to the IMGT nomenclature (Lefranc et al., 2003). (b) Biolayer interferometry (BLI) association and dissociation curves for indicated concentrations of Fab B11 (black) binding to immobilized p67. Binding signals were globally fit (gray) and the calculated K_D value is shown. (c) ELISA for binding (*y*-axis) of serial dilutions of Fab B11 (*x*-axis) to His-p67C (black squares) and the negative control proteins ubiquitin (white circles) and BSA (white triangles). (d) ELISA for binding (*y*-axis) of 50 nM Fab B11 (black), IgG AR21.4 (gray), and IgG AR22.7 (white) to the following antigens (*x*-axis): Full-length p67, p67N (residues 21–225), and p67C (residues 572–651). (e) ELISA for binding (*y*-axis) of 50 nM Fab B11 (black) and IgG AR21.4 (gray) to the following antigens (*x*-axis): p67C, $p67^1$, and $p67^2$. (f) Neutralization activity in an in vitro sporozoite neutralization assay with bovine PBMCs. Five-fold serial dilutions of antibody from 250 nM were evaluated in the sporozoite neutralization assay relative to a non-binding IgG isotype control. Error bars were derived from the standard deviation of technical replicates run in triplicate and results shown are representative of experiments run in quadruplicate.

Nene et al., 1999) for neutralizing activity in a sporozoite neutralization assay (Chege et al., 2024), relative to a non-neutralizing isotype control IgG. Following a 30-minute pre-incubation with sporozoite, anti-p67 Ab prevented the infection of bovine peripheral blood mononuclear cells (PBMCs) as determined by flow cytometric analysis, while the control antibody showed no evidence of neutralization at any concentration. Both IgGs exhibited essentially complete sporozoite neutralization at ~50 nM, while only ~30% inhibition was achieved by Fab B11 at the same concentration. Approximation of potencies by parametric fitting of neutralization data resulted in IC_{50} values for IgGs B11 and 21.4 in the 15–20 nM range, while Fab B11 neutralized with roughly 10-fold less potency, though the exact values were not determined due to incomplete fitting of the data (Figure 1f).

2.4 | The crystal structure of fab B11 in complex with $p67C^1$ reveals a discrete epitope

Having used binding studies with recombinant protein fragments to narrow the epitope for Fab B11 to the 41-residue fragment $p67^1$ (Figure 1e), we solved the crystal structure of the Fab-B11:p67C (Nene & Morrison, 2016) complex at a resolution of 2.0 Å with an R_{work} and R_{free} of 20.3% and 26%, respectively (Figure 2 and Table 1). The crystals grew in space group P1 with two Fab:peptide complexes in the asymmetric unit. The two complexes were highly similar, with an average backbone root mean square deviation (RMSD) of 0.35 Å, so only one of the complexes is described here.

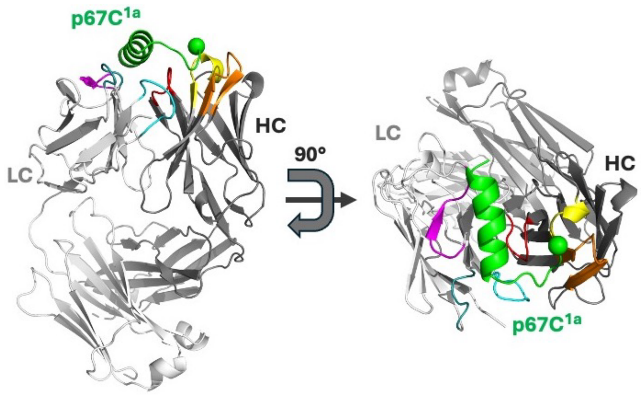

FIGURE 2 Crystal structure of Fab B11 in complex with p67C[1]. (a) Fab B11 is shown as a ribbon with the light chain (LC) and heavy chain (HC) colored light or dark gray, respectively, except for the CDRs (as defined by the IMGT nomenclature (Lefranc et al., 2003)), which are colored as follows: L1, (blue), L2 (magenta), L3 (cyan), H1 (yellow), H2 (orange), H3 (red). p67C[1a] (the 20-residue region of p67C (Nene & Morrison, 2016) that was resolved in the electron density map) is shown as a green ribbon with the N-terminus rendered as a sphere. The side and top-down views of Fab B11 are shown at left and right, respectively.

The model comprised residues 1–212 and 2–217 of the Fab light and heavy chains, respectively, and residues 579–598 of the p67[1] peptide (Figure 2). Although the peptide used in the crystallization contained 41 residues, only 20 residues were visible in the electron density map, and we speculate that the unresolved residues at either end of the peptide do not interact with the Fab and are disordered in the crystal. The C-terminal region (residues 585–598) of the visible peptide forms an *α*-helix that resides within a cleft between the VH and VL domains, whereas the N-terminal region (residues 580–583) forms a *β*-turn that interacts with the heavy chain CDRs. The C-terminal region was also predicted to form an *α*-helix in several secondary structure prediction algorithms, including AlphaFold.

TABLE 1 Data collection and refinement statistics for the crystal structure of the Fab-B11:p67[1] complex.

Protein complex	Fab B12/p67C[1]
PDB ID	8UX6
Data collection	
Beam line	NECAT-24-ID-E
Wavelength (Å)	0.97918
Crystal	Native
Unit cell parameters	
Space group	P1
a, *b*, *c* (Å)	39.0, 75.6, 90.6
α, *β*, *γ* (°)	69.3, 77.6, 76.1
Diffraction data	
Resolution (Å)	83.85–2 (2.05–2.00)[a]
Unique reflections	64,860 (4175)
Completeness (%)	87.3 (88.5)
Rpim	0.059 (0.241)
Overall I/σI	7.8 (3.4)
Multiplicity	2.2 (2.2)
Wilson B-factor	29.2
Refinement statistics	
Resolution (Å)	19.52–2.00
Rwork/Rfree	0.204/0.251
RMSD bond lengths (Å)	0.008
RMSD bond angles (°)	0.94
Number of protein atoms	6556
Number of water atoms	498
Number of other atoms	148
B-factor average	42.4
B-factor macromolecules	42.2
B-factor water	41.9
B-factor other	51.8
Ramachandran statistics (molprobity)	
Preferred (%)	97.5
Allowed (%)	2.5
Disallowed (%)	0
Clash score	7.4

[a]Values in parentheses represent highest-resolution shells.

2.5 | Binding assays with synthetic peptides define minimal epitopes for Fab B11 and IgGs AR21.4 and AR22.7

Structural analysis suggested that only a small number of residues within a 20-residue stretch of p67 (residues 579–598) made contacts with Fab B11 (Figure 2). We hypothesized that this 20-residue peptide, which we named p67C[1a], should be sufficient to bind to Fab B11 with the same affinity as full-length p67. To test this hypothesis, we established a BLI assay that used immobilized biotinylated peptides representing the antigen to measure interactions with solution-phase Fab B11. We synthesized a biotinylated 25-residue peptide encompassing residues 574–598 of the antigen (5 residues were added to the N-terminus to obviate steric hinderance from the sensor surface), and we confirmed high-affinity binding ($K_D = 22$ nM, Figure 3a). Insofar as binding to the peptide is several-fold better than to the full-length p67 ($K_D = 79$ nM, Figure 1b), it suggests that the structure of functionally folded, full-length surface protein may pose a modest steric obstacle to binding.

We also used BLI to estimate affinities and validate peptide epitopes for the previously reported neutralizing IgGs AR21.4 (Figure 3b) and AR22.7 (Figure 3c). In this case, we took advantage of previously reported qualitative binding data with peptide arrays (Nene et al., 1999)

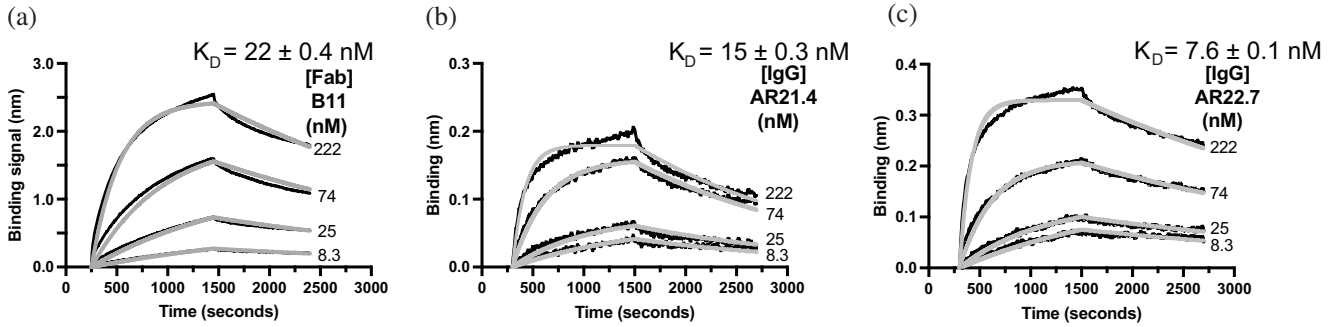

FIGURE 3 Antibodies binding to minimal p67 epitopes. (a) Fab B11 binding to p67 residues 574–598 (biotin-GGGSLRGLDLSEEEVKKILDEIVKD). (b) IgG AR21.4 binding to p67 residues 612–628 (PSGRSSERQPSLGPSLVGGGSK-biotin). (c) IgG AR22.7 binding to p67 residues 204–220 (ELKKTLQPGKTSTGETTGGGSK-biotin). BLI association and dissociation curves (black) are shown for indicated concentrations (black) of antibody binding to immobilized biotinylated peptide. Binding signals were globally fit (gray) and the calculated K_D values are shown.

to identify 17-residue peptides predicted to bind to IgG AR21.4 (residues 612–628, PSGRSSERQPSLGPSLV) or IgG AR22.7 (residues 204–220, ELKKTLQPGKTST-GETTS). Peptides were designed based on the 2 overlapping peptides described in Nene et al. (1999) by combining the overlapping 7-mer regions of the two peptides into a single peptide with an additional 5 native amino acids on either end and a biotinylated G4S linker on the N-terminal end. Each chimeric IgG bound with high affinity to its cognate peptide (K_D = 15 and 7.5 nM for AR21.4 or AR22.7, respectively) (Figure 3b, c) and exhibited no detectable binding to non-cognate peptides (data not shown). Taken together, these results reveal that Fab B11 and IgGs AR21.4 and AR22.7 recognize three distinct, short peptide epitopes, each of which can be targeted to neutralize infection by *T. parva* sporozoites.

2.6 | Alanine-scanning reveals critical binding residues of the Fab B11 epitope

We used the BLI assay to systematically quantify the contribution of each residue within p67C^{1a} to the energetics of the binding interaction with Fab B11. We conducted an alanine scan of p67C^{1a} using a panel of peptides in which each peptide contained an alanine substitution in place of one of the 20 residues, as alanine substitutions have been shown to give a good measure of the contribution of each side chain to binding without perturbing mainchain conformations (Wright & Lim, 2001).

The alanine-scan data were used to compute the ratios (Ala/WT) of the K_D values for each alanine analog compared with the WT peptide (Table 2). Notably, none of the ratios were significantly <1, indicating that there are no significant negative interactions between

TABLE 2 Binding kinetics for alanine-substituted p67C^{1a} variants binding to Fab B11[a].

Variant[b]	Ratio (Ala/WT)[c]	^{K}D (nM)	^{k}on (10^3 $M^{-1}s^{-1}$)	k_{off} (10^{-4} s^{-1})
WT	1	22 ± 1	15 ± 1	3.3 ± 1
R579A	1.4	31 ± 1	27 ± 1	8.0 ± 1
G580A	110	2400 ± 260	18 ± 1	440 ± 30
L581A	>1000	NBD	NBD	NBD
D582A	4.3	94 ± 2	14 ± 1	14 ± 1
L583A	9.1	200 ± 5	7.3 ± 1	15 ± 1
S584A	7.3	160 ± 4	7.2 ± 1	11 ± 1
E585A	4.2	93 ± 2	15 ± 1	14 ± 1
E586A	1.9	43 ± 1	27 ± 1	11 ± 1
E587A	5	110 ± 3	13 ± 1	14 ± 1
V588A	>1000	NBD	NBD	NBD
K589A	11	250 ± 8	9.0 ± 1	23 ± 1
K590A	2.5	53 ± 1	24 ± 1	13 ± 1
I591A	3.4	74 ± 2	16 ± 1	12 ± 1
L592A	>1000	NBD	NBD	NBD
D593A	>1000	NBD	NBD	NBD
E594A	1.2	27 ± 1	37 ± 1	10 ± 1
I595A	0.9	20 ± 1	34 ± 1	7 ± 1
V596A	2.1	47 ± 1	29 ± 1	14 ± 1
K597A	91	2000 ± 140	4.7 ± 1	96 ± 1
D598A	4.8	106 ± 4	24 ± 1	25 ± 1
P599A	0.9	20 ± 1	39 ± 1	7.9 ± 1
S600A	2.3	51 ± 1	24 ± 1	12 ± 1
D601A	1.6	36 ± 1	29 ± 1	11 ± 1

[a]Binding kinetics were determined by BLI with biotinylated peptides immobilized on streptavidin-coated tips and Fab B11 in solution. The globally fit K_D, k_{on}, and k_{off} values are reported with errors from a 7-point, 3-fold dilution series of Fab from 2000 to 2.7 nM.
[b]Variants were represented by synthetic peptides in the context of the following WT peptide: biotin-GGGSLRGLDLSEEEVKKILDEIVKD.
[c]The Ala/WT ratio was determined from the respective K_D values.

the Fab and antigen. However, six alanine substitutions had a significant negative impact on binding (Ala/WT >90), indicating that the corresponding six residues contribute favorably to the interaction. Alanine substitutions for four residues (Leu^{581}, Val^{588}, Leu^{592}, Asp^{593}) had a major impact on affinity, as evidenced by no detectable binding in the assay (Ala/WT >1000), and for two other residues (Gly^{580} and Lys^{597}), alanine substitutions had a moderate impact on affinity (Ala/WT = 110 or 91, respectively). Thus, these results show that within the small 20-residue peptide p67C^{1a}, an even smaller subset of six residues contributes most of the binding energy for the Fab B11 paratope.

2.7 | Mapping the functional epitope on the structural epitope

To visualize the functional epitope within p67C^{1a}, we mapped the alanine-scanning results onto the structure of the Fab-B11:p67C^{1a} complex (Figure 4a). The complex of Fab B11 with p67C^{1a} results in the burial of a total of 1531 Å^2 of surface area, with 721 and 810 Å^2 on the antibody and antigen side, respectively. The structural paratope of Fab B11 is evenly divided between the light and heavy chains, which contribute 342 Å^2 (47.4%) and 379 Å^2 (52.6%) of buried surface area, respectively. Within this extensive interface, there are myriad hydrophobic and hydrophilic interactions that together explain the high affinity and specificity of the interaction.

Within the 721 Å^2 structural epitope on p67C^{1a}, the functional epitope consisting of the six residues that were hits in the alanine-scan represents a much smaller buried surface area of 398 Å^2. This functional epitope contains two hydrophobic clusters that interact with the Fab B11 paratope (Figure 4a). In one cluster, the peptide adopts a loop conformation, and Gly^{580} presses against the side chains of Ser^{57H} and Tyr^{62H}. Gly is the only amino acid that is smaller than Ala, and an alanine substitution at this position could cause a steric clash. Leu^{581} resides in a pocket containing the side chains of Ser^{55H}, Ser^{57H}, Ser^{64H}, Ser,^{66H} and Tyr113^{H}, and the main chain atoms of Ile^{56H} and Thr^{65H} (Figure 4b-i). The complete abrogation of binding observed upon mutation of Leu^{581} to Ala (Table 2) suggests that these interactions are critical. Following the loop and beginning at residue Glu^{585}, the peptide adopts a helical conformation, and the second hydrophobic cluster consists of Val^{588} and Leu^{592}, which interact with residues in CDR-H3 (Pro^{108H}, Gly^{109H}, Ala^{114H}) and the light chain (Tyr^{68L} and Tyr^{107L}) through complementary burial of hydrophobic side chains (Figure 4b-ii). Mutation of either Val^{588} or Leu^{592} to Ala also eliminated binding of the peptide by Fab B11, further confirming the importance of these residues and the energy that hydrophobic interactions contribute to the overall peptide-binding landscape. The remaining two residues (Asp^{593} and K^{597}) in the functional epitope are hydrophilic, and they reside on a largely solvent-exposed face of the helix (Figure 4b-iii). The side chain of Asp^{593} makes a hydrogen bond with the side chain of Tyr^{55L}. In contrast, Lys^{597} does not interact with Fab B11, and we could not model the electron density beyond the gamma carbon of the side chain. While the complete loss of binding observed upon mutation of Asp^{593} to Ala supports the importance of this interaction, the strong impairment of binding observed when Lys^{597} is mutated to Ala was not predicted from the structure. However, as mentioned, the C-terminal region of p67 including residues 585–598 has a strong helical propensity. We speculate that the periodicity of the oppositely charged Asp^{593} and Lys^{597} residues may be important for stabilizing the helix, and substitution of either residue with alanine may result in a greater energetic cost for the peptide to adopt a helical conformation that positions the hydrophobic side chains on the opposite face of the helix for favorable interactions with Fab B11.

Taken together, our structural and functional analyses define a short and discrete neutralizing epitope within p67, consisting of a 20-residue peptide within which five side chains make contacts that contribute most of the binding energy with the Fab B11 paratope.

3 | DISCUSSION

We have identified a discrete, neutralizing epitope comprised of *T. parva* p67 residues 579–598 by structural characterization of a 41-residue polypeptide in complex with the neutralizing, synthetic Fab B11. While immunization of cattle with p67C—an 80-residue C-terminal fragment of p67—has been shown previously to elicit neutralizing antibodies and provide immune protection against *T. parva* (Lacasta et al., 2018, 2021), there are limited reports of well-characterized, sporozoite-neutralizing antibodies with defined epitopes (Nene et al., 1999) to inform epitope-directed, subunit vaccine development efforts. The detailed characterization of a novel neutralizing antibody and its epitope—and the validation of two other recombinant antibodies targeting neutralizing epitopes (IgGs AR22.7 and AR21.4)—provides an important set of tools to support this aim.

Previous studies reported a non-neutralizing murine mAb (38.9) that targeted peptide pin 75 (^{585}EEEVKKILDEIVKDP^{599}) (Nene et al., 1999) as well as sera from cattle that were immune to ECF and targeted peptide pin 74 (^{577}SLRGLDLSEEEVKKI^{591}). Notably, this confirms that the epitopes of both mAbs and immune sera can overlap with the epitope for Fab B11 (^{580}GLDLSEEEVKKILDEIVKD^{598}) determined in this study (Nene et al., 1999). However, peptide-binding studies such as these, generally conducted at 25°C,

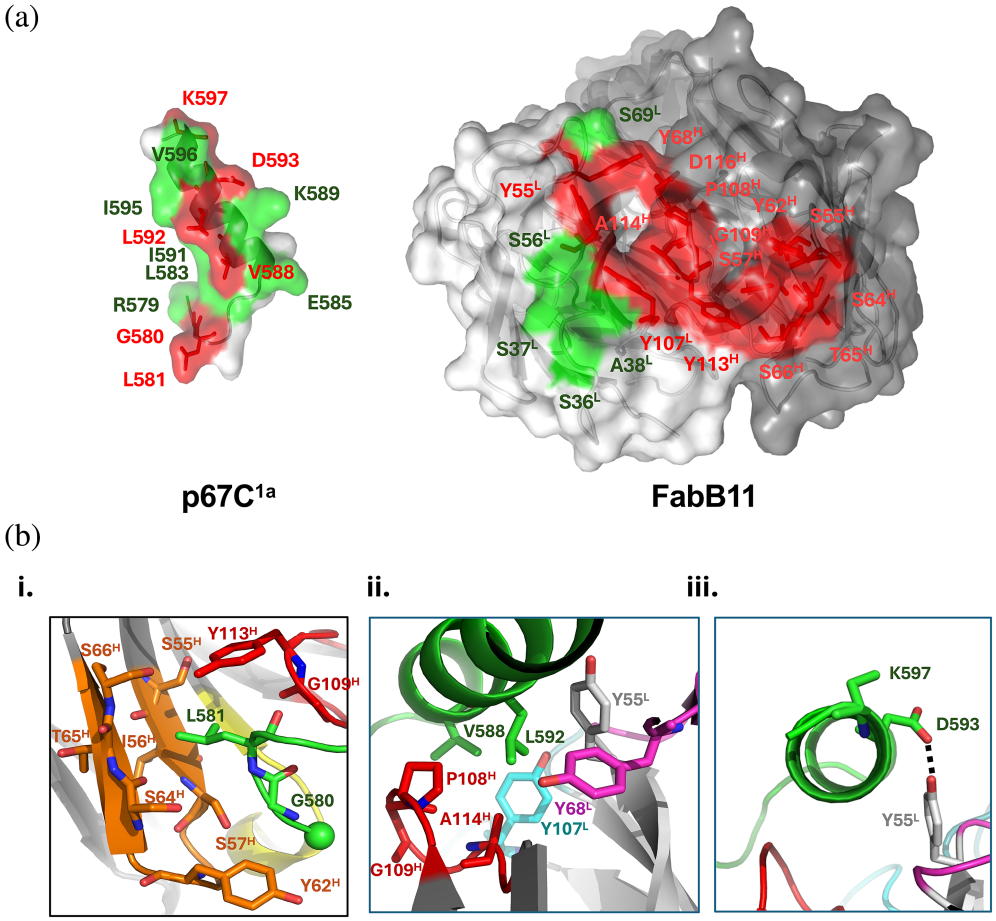

FIGURE 4 The functional epitope of p67C^{1a} for binding to Fab B11. (a) Open book view of the p67C^{1}:Fab-B11 complex. The 20-residue p67C^{1a} peptide (left) and Fab B11 (right) are shown as transparent surfaces. p67C^{1a} residues are colored red or green if alanine substitutions did or did not reduce binding significantly (Ala/WT >6), respectively, and residues that do not contact Fab B11 are colored gray. Side chains are shown for residues that were hits in the alanine scan. Fab B11 residues are colored red or green if they contact p67C^{1a} residues that were or were not hits in the alanine scan, respectively, and other residues in the light and heavy chains are colored light or dark gray, respectively. Side chains are shown for residues that contact p67C^{1a} residues that were hits in the alanine scan. (b) Details of the molecular interactions between Fab B11 and p67C^{1a} residues (i) G^{580} and Leu^{581}, (ii) Val^{588} and Leu^{592}, and (iii) Asp^{593} and K^{597}. p67C^{1a} residues are colored green. Fab B11 residues are colored as follows: CDR-L2, (magenta), CDR-L3 (cyan), CDR-H1 (yellow), CDR-H2 (orange), CDR-H3 (red), framework (gray). Fab B11 side chains that interact with the relevant p67C^{1a} residues are shown, and hydrogen bonds are shown as dashed lines.

are only intended to show binding, estimate critical interactions, and validate structural findings, and apparent binding under physiological conditions has not been determined. While the key infective stages of the functional assay herein were conducted at 37°C, thus supporting the primary finding—that blockade of this epitope is effective in reducing infection in vitro—additional studies are required to contextualize and validate these findings in vivo toward the aim of translation. Together, the observations above suggest only that the bovine humoral immune response to sporozoite infection can generate immunoreactivity that overlaps with that of a synthetic antibody to the same region that neutralizes sporozoite infection in vitro.

Thus, it remains an open question (1) whether the Fab B11 epitope is a bona fide target of neutralizing antibodies generated during the in vivo bovine humoral response and (2) whether this peptide identified as the target of Fab B11 can elicit a protective immune response. First, further studies are required to determine conclusively whether bovine antibodies generated following in vivo immune challenge with p67C do indeed target a region overlapping with this epitope. By isolating clonal bovine anti-p67 IgGs and verifying whether their epitopes overlap, this could enable functional characterization of those antibodies and whether they contribute to the in vivo neutralization of sporozoite challenge, which would further need to be demonstrated. In laboratory stocks of *T. parva* derived from cattle and used to generate antigens for study and immunization, p67 expressed in the sporozoites has been determined to be invariant (Nene et al., 1996) and thus, immune sera and isolated bovine antibodies derived from inoculation are useful biological samples

for exploring these questions. However, *T. parva* isolates from cattle populations in some regions of Africa do exhibit sequence diversity in p67 (Mukolwe et al., 2020), and buffalo populations constitute a reservoir of *T. parva* diversity that can readily cross the species barrier. These sources of natural diversity must also be considered in any sort of binding/neutralization study. Second, it has not yet been established whether the 20-mer peptide identified can indeed trigger a neutralizing immune response in vivo independently of the p67C immunogen. Though immunization of cattle with a naked or adjuvanted synthetic peptide may not be feasible or cost-effective at this time, our in vitro results do support additional translational studies aimed at determining modalities of peptide presentation that could be effective in eliciting a robust immune response, including expansion of both B and T cells specific for the peptide antigen. The limited efficacy of immunization with recombinant p67C has led to the idea that epitope display in a more ordered manner through use of nanoparticles could enhance immunity (Lacasta et al., 2021; Xu et al., 2023), and a series of non-overlapping peptide epitopes with potential to elicit bovine immune responses, as discussed here, could aid in devising innovative multivalent, peptide-nanoparticle display strategies for immunization. While this is a substantial effort to bridge the translational gap between our work and an effective addition to an experimental peptide-directed vaccine, studies are currently underway to investigate these questions.

Similar approaches that use (poly)peptide epitopes known to be targeted by neutralizing antibodies have been employed to develop vaccines for other parasites. In individuals immunized with the circumsporozoite protein PfCSP of *Plasmodium falciparum*, the parasite that causes malaria, the most potent neutralizing antibodies target repeat regions found in the structurally disordered central region and confer protection from parasitemia in experimental animal models (Murugan et al., 2020). Two vaccines that display extended segments comprised of both these repeat motifs and the C-terminal region of CSP coupled to a synthetic immunogen have been shown to induce a protective immune response (Anon, 2015; Datoo et al., 2024). While these vaccines are now authorized for use and expected to impact the malarial burden, neither produce sterilizing immunity. Further, disparities in efficacy and durability of protection between the two vaccines, suggest that gaps in our understanding persist and further improvements are needed. An experimental vaccine using a discrete 15-residue peptide derived from the junction between the N-terminal and central repeat regions of PfCSP provided long-lasting though non-sterilizing immunity in animal models of infection, suggesting possible ways in which additional non-repeat peptidic regions may enhance efficacy and/or durability in existing epitope-based vaccines (Jelínková et al., 2021).

The surface proteins of other parasites targeted by neutralizing antibodies have also been used to develop peptide-based vaccines that have shown experimental efficacy against *Leishmania* (Petitdidier et al., 2019), *Schistosoma* (Arnon et al., 2000) and *hookworm* (Bartlett et al., 2020) *infections*, suggesting the broad applicability of this approach. The addition of a third putative neutralizing epitope within the p67C polypeptide and an antibody that can be used to validate its targeting provide impetus and tools for continued investigation of the potential utility of an experimental peptide-based vaccine for *T. parva*.

4 | METHODS AND MATERIALS

4.1 | Production of p67 proteins

A DNA fragment encoding full-length p67 with a C-terminal His-tag (Genscript) was cloned into a pSCST mammalian expression vector using restriction-free cloning methods. HEK Expi293 cells were transiently transfected with the expression plasmid using FECTO-Pro reagent (Polyplus transfection) following the manufacturer's protocol. After 5 days, the cell media was harvested, and p67 protein was purified by affinity chromatography using Ni-NTA beads. The protein preparations were analyzed by SDS-PAGE to assess identity and homogeneity and stored at −80°C.

The DNA fragments encoding for p67C, p67C^{1}, and p67C^{2} were purchased as gblocks (IDT, Iowa) and cloned into the pHH0103 bacterial expression vector (Teyra et al., 2017) with N-terminal GST/6XHis fusion tags (with a TEV cleavage site between the two tags) using restriction-free cloning methods (Van Den Ent & Löwe, 2006). Sequence-verified plasmids were transformed into *Escherichia coli* BL21 (DE3) cells (Novagen) and grown at 37 °C in 2YT media supplemented with 100 μg/mL carbenicillin until they reached mid-log phase, at which point protein production was induced with 0.5 mM IPTG (CAR666.5, Bioshop) and the cultures were grown overnight at 18°C with shaking. Cells were harvested and lysed in lysis buffer (25 mM Tris (pH 7.5), 150 mM NaCl, 20 mM imidazole, 5 mM 2-mercaptoethanol) by repeated freeze–thaw cycles, then clarified from cell debris by centrifugation at 30,000 × *g* at 4°C for 40 min before purification using Glutathione Sepharose 4B (GE17-0756-05, Sigma) followed by on-column cleavage of the GST-tag with TEV protease (where necessary) in the same buffer. Protein preparations were assessed for purity and homogeneity by SDS-PAGE and stored at −80°C.

4.2 | Production of Fab B11 protein

DNA fragments encoding the variable domains of Fab B11 were cloned into the RH2.2 *Escherichia coli*

expression vector using standard molecular biology techniques, and a sequence-validated construct was transformed into *E. coli* BL21 (DE3) cells (Novagen). A culture harboring the expression plasmid was grown in 2YT media supplemented with 100 μg/mL carbenicillin to mid-log phase, at which point, protein production was induced by the addition of 1 mM IPTG (CAR666.5, Bioshop), and the culture was grown overnight at 28°C with shaking at 200 rpm. Cells were pelleted by centrifugation, frozen at −80°C for 30 min, resuspended in lysis buffer (PBC, 1% (V/V) Triton X-100, 2.5 U/mL benzonase (71206–03, Novagen), 2 mM MgCl2, 0.2 mM PMSF, 1 mg/mL lysozyme (LYS702.1, Bioshop)), and gently nutated for 2 hours at 4°C. Lysate was cleared at 20,000 × *g* for 30 min, and Fab protein was purified with rProtein A Sepharose® Fast Flow (GE Healthcare) following a 2 h incubation at 4°C with shaking. The beads were washed with 40 mL PBS, and protein was eluted with elution buffer (50 mM NaH_2PO_4, 100 mM H_3PO_4, 140 mM NaCl, pH 2.8) and neutralized with 1 M Bis-tris propane-HCl, pH 11.0. Protein yield and purity were determined by OD_{280} measurement and visualization on a Coomassie-stained SDS-PAGE gel.

4.3 | Production of chimeric IgG proteins

The amino acid sequences of the variable heavy and light chain regions of mouse antibodies AR21.4 and AR22.7 were reverse translated and DNA fragments encoding the variable regions were synthesized (Twist Bioscience) and cloned into the corresponding regions of the pSCSTa human Ig1 and *hκ* vectors, respectively. The resultant constructs were amplified, purified, and transfected into Expi293 cells as described previously for IgG expression (Miersch et al., 2022). Expressed human IgG1 protein was purified by affinity chromatography with Protein A Sepharose (17127904, Cytiva) and buffer exchanged and concentrated using Amicon Ultra-15 Centrifugal Filter devices (UFC805096, Millipore).

4.4 | Phage display selections

The phage-displayed synthetic Fab library (Persson et al., 2013) was cycled through 4 rounds of binding selections with p67C immobilized on 96-well plates (M9410-1CS, Thermo Scientific), as described (Fellouse & Sidhu, 2006). After the fourth round, 96 individual phage clones were amplified and analyzed by phage ELISA. Clones that bound to p67C but not to negative control proteins (ubiquitin and BSA) were subjected to DNA sequence analysis to decode the sequences of the Fab variable domains.

4.5 | Sporozoite neutralization assay

Recombinant antibodies Fab B11, IgG B11, and IgG AR21.4 were tested for their ability to inhibit the in vitro infectivity of *T. parva* sporozoites alongside irrelevant human IgGs using a seroneutralization assay, as previously described with slight modifications (Chege et al., 2024). Briefly, antibodies serially diluted 5-fold from 250 to 0.0032 nM were pre-incubated with sporozoites from batch 25/24 diluted at 1 in 5 in complete RPMI for 30 min. The sporozoite/antibody mixture was added to bovine PBMCs and incubated for 12 days at 37°C in 5% CO_2. Infected cells were detected by anti-PIM staining and FACS analysis, and the results were expressed as the percentage of neutralization compared to the level of infection without antibodies.

4.6 | ELISAs

Antigen or negative control proteins (5 μg/mL in PBS) were immobilized overnight at 4°C with shaking in microwell plates (M9410-1CS, Thermo Scientific). Fab-phage, Fab proteins, and IgG proteins were used as primary reagents, as described (Birtalan et al., 2008), and binding signals were detected with HRP-fused anti-M13 (27-9421-01, GE Healthcare), anti-FLAG M2 (F1804-50UG, Sigma), or anti-Fc (AB_2337579, Jackson Immunoresearch) secondary antibodies, as appropriate. Plates were washed 8 times between each step using PBS supplemented with 0.25% Tween 20. The reaction was developed for 2 min with TMB substrate (KP-50-76-03, Mandel) and stopped with 1.0 M phosphoric acid. Absorbance was read at a 450 nm wavelength on an H1 Synergy plate reader (Biotek).

4.7 | Biolayer interferometry

BLI was used to measure the binding kinetics (k_{on} and k_{off}) of Fab B11 for p67 and its derivative peptides. Full-length p67 protein (0.2 μM in PBS) was immobilized on an AR2G sensor (ForteBio). Biotinylated peptides (Custom, Abclonal) were immobilized on streptavidin capture (SA) sensors (ForteBio) at various concentrations (1.2, 0.12, and 0.04 μM) to control for surface crowding effects and avidity. A 3-fold dilution series of 2 μM Fab B11 or a negative control Fab was prepared in assay buffer (PBS, 1% BSA, 0.05% Tween 20), and following equilibration with assay buffer, loaded biosensors were dipped for 600 seconds into protein- or peptide-coated wells and subsequently transferred back into assay buffer for 600 s. Binding response data were corrected by subtraction of the response from either a non-binding control Fab or non-binding biotinylated control peptide and fitted with a 1:1 binding model using ForteBio Octet Systems software 9.0.

4.8 | Crystallization and data collection

Fab B11 protein was purified using Protein A Sepharose and concentrated to 14 mg/mL. Fab protein was incubated with polypeptide at a 1:1.1 molar ratio for 2 h at 4°C. The Fab-B11:p67C[1] complex was subjected to gel filtration on a Superdex 75 16/600 GL column (GE Healthcare) and equilibrated in 20 mM HEPES pH 7.5, 150 mM NaCl. The purity of the Fab-B11:p67[1] complex was assessed by SDS-PAGE of relevant purification fractions, which were then concentrated to 12 mg/mL using Amicon Ultra-4 filters (Millipore; UFC810024), flash frozen in 100 μL aliquots in liquid nitrogen, and stored at −80°C. The Fab-B11:p67[1] complex was subjected to crystallization screening with several commercial 96-well screens using the Mosquito LCP crystallization robot (SPT LabTech). Initial hits were obtained from the GRAS2 screen (Hampton Research, Aliso Viejo, CA). Needle-like crystals appeared in multiple different conditions after several days, and these were further optimized for size and shape. For structure determination, crystals were obtained from 0.1 M HEPES, pH 7 containing 25% PEG 6000 (w/v) and 0.2 M $CaCl_2$. The crystals were cryoprotected by equilibration in a similar buffer containing 20% ethylene glycol, followed by flash-freezing in liquid nitrogen. Diffraction data were collected at a wavelength 0.97918 Å using Argonne National Laboratories (Chicago) beamline 24-ID-E (NE-CAT). Data were integrated with MOSFLM (Battye et al., 2011) and scaled and merged with AIMLESS (Anon, 1994).

4.9 | Structure determination

The structure of the Fab-B11:p67C[1] complex was determined by molecular replacement using a SWISS-MODEL model of the Fab heavy and light chains. Molecular replacement was performed with PHASER (McCoy et al., 2007) within the PHENIX Crystallography suite (Adams et al., 2002) with the variable and constant domains of the heavy and light chains used as individual search models (Table 1). Following molecular replacement, significant difference density could be observed for all Fab domains and for the peptide, which was modeled using the graphics package COOT (Emsley & Cowtan, 2004). Refinement of the model was carried out by Phenix. refine within the PHENIX suite and COOT, in the PHENIX suite, which included water picking. Finally, TLS parameters were generated from the Fab-B11:p67C (Nene & Morrison, 2016) complex coordinates (Painter & Merritt, 2006) and used during refinement (Urzhumtsev & Afonine, 2013). The final model contained good geometry with a low clashscore, and no backbone dihedrals were found in the disallowed or unfavorable region of the Ramachandran Plot.

AUTHOR CONTRIBUTIONS

Shane Miersch: Investigation; writing – original draft; supervision; data curation; project administration; writing – review and editing; validation. **Alex U. Singer:** Investigation; validation; writing – review and editing. **Chao Chen:** Investigation. **Fred Fellouse:** Investigation. **Anupriya Gopalsamy:** Investigation. **Luciano Silva e Costa:** Investigation. **Anna Lacasta:** Investigation; writing – review and editing; methodology. **Hannah Chege:** Investigation. **Naomi Chege:** Investigation. **Vishvanath Nene:** Investigation; writing – review and editing; supervision; conceptualization. **Sachdev S. Sidhu:** Investigation; funding acquisition; writing – review and editing; supervision; conceptualization.

ACKNOWLEDGMENTS

We thank Igor Kurinov at NE-CAT, Department of Chemistry and Chemical Biology, Cornell University, Argonne, IL 60439, USA, for data collection. This work was supported by funds from the International Development Research Centre Joint Canada-Israel Health Research Program #108404-001 and the Canada Foundation for Innovation Physical Infrastructure Grant #33363 to S.S.S. as well as funds from the Bill and Melinda Gates Foundation's East Coast Fever Research Consortium, Global Development Grant #OPP1078791, Subgrant ECF06/2014 to V.N.

DATA AVAILABILITY STATEMENT

The data that support the findings of this study are available from the corresponding author upon reasonable request.

REFERENCES

Adams PD, Grosse-Kunstleve RW, Hung LW, Ioerger TR, McCoy AJ, Moriarty NW, et al. PHENIX: building new software for automated crystallographic structure determination. Acta Crystallogr D Biol Crystallogr. 2002;58:1948–54.

Anon. The CCP4 suite: programs for protein crystallography. Acta Crystallogr D Biol Crystallogr. 1994;50:760–3.

Anon. Efficacy and safety of RTS,S/AS01 malaria vaccine with or without a booster dose in infants and children in Africa: final results of a phase 3, individually randomised, controlled trial. Lancet. 2015;386:31–45.

Arnon R, Tarrab-Hazdai R, Steward M. A mimotope peptide-based vaccine against Schistosoma mansoni: synthesis and characterization. Immunology. 2000;101:555.

Bartlett S, Eichenberger RM, Nevagi RJ, Ghaffar KA, Marasini N, Dai Y, et al. Lipopeptide-based Oral vaccine against hookworm infection. J Infect Dis. 2020;221:934–42.

Battye TGG, Kontogiannis L, Johnson O, Powell HR, Leslie AGW. iMOSFLM: a new graphical interface for diffraction-image processing with MOSFLM. Acta Crystallogr D Biol Crystallogr. 2011;67:271–81.

Birtalan S, Zhang Y, Fellouse FA, Shao L, Schaefer G, Sidhu SS. The intrinsic contributions of tyrosine, serine, glycine and arginine to the affinity and specificity of antibodies. J Mol Biol. 2008;377:1518–28.

Bishop R, Nene V, Staeyert J, Rowlands J, Nyanjui J, Osaso J, et al. Immunity to East Coast fever in cattle induced by a polypeptide

fragment of the major surface coat protein of *Theileria parva* sporozoites. Vaccine. 2003;21:1205–12.
Chege H, Githigia S, Gathumbi J, Chege N, Ojuok R, Odaba J, et al. An improved *Theileria parva* Sporozoite Seroneutralization assay for the identification of East Coast fever immune correlates. Antibodies. 2024;13:100.
Datoo MS, Dicko A, Tinto H, Ouédraogo JB, Hamaluba M, Olotu A, et al. Safety and efficacy of malaria vaccine candidate R21/-matrix-M in African children: a multicentre, double-blind, randomised, phase 3 trial. Lancet. 2024;403:533–44.
Emsley P, Cowtan K. Coot: model-building tools for molecular graphics. Acta Crystallogr D Biol Crystallogr. 2004;60:2126–32.
Fellouse F, Sidhu SS. Making antibodies in bacteria. Making and using antibodies. Boca Raton: CRC Press; 2006. p. 171–94.
Gharbi M, Darghouth MA. Control of tropical theileriosis (*Theileria annulata* infection in cattle) in North Africa. Asian Pac J Trop Dis. 2015;5:505–10.
Jelínková L, Jhun H, Eaton A, Petrovsky N, Zavala F, Chackerian B. An epitope-based malaria vaccine targeting the junctional region of circumsporozoite protein. NPJ Vaccines. 2021;6:13.
Lacasta A, Kim HC, Kepl E, Gachogo R, Chege N, Ojuok R, et al. Design and immunological evaluation of two-component protein nanoparticle vaccines for East Coast fever. Front Immunol. 2023;13:1015840.
Lacasta A, Mody KT, de Goeyse I, Yu C, Zhang J, Nyagwange J, et al. Synergistic effect of two nanotechnologies enhances the protective capacity of the *Theileria parva* Sporozoite p67C antigen in cattle. J Immunol. 2021;206:686–99.
Lacasta A, Mwalimu S, Kibwana E, Saya R, Awino E, Njoroge T, et al. Immune parameters to p67C antigen adjuvanted with ISA206VG correlate with protection against East Coast fever. Vaccine. 2018;36:1389–97.
Lefranc MP, Pommié C, Ruiz M, Giudicelli V, Foulquier E, Truong L, et al. IMGT unique numbering for immunoglobulin and T cell receptor variable domains and Ig superfamily V-like domains. Dev Comp Immunol. 2003;27:55–77.
McCoy AJ, Grosse-Kunstleve RW, Adams PD, Winn MD, Storoni LC, Read RJ. Phaser crystallographic software. J Appl Cryst. 2007; 40:658–74.
Miersch S, Sharma N, Saberianfar R, Chen C, Caccuri F, Zani A, et al. Ultrapotent and broad neutralization of SARS-CoV-2 variants by modular, tetravalent, bi-paratopic antibodies. Cell Rep. 2022;39:110905.
Mukolwe LD, Mukolwe LD, Odongo DO, Byaruhanga C, Byaruhanga C, Snyman LP, et al. Analysis of p67 allelic sequences reveals a subtype of allele type 1 unique to buffalo-derived *Theileria parva* parasites from southern Africa. PLoS One. 2020;15:e0231434.
Murugan R, Scally SW, Costa G, Mustafa G, Thai E, Decker T, et al. Evolution of protective human antibodies against *Plasmodium falciparum* circumsporozoite protein repeat motifs. Nat Med. 2020;26:7.
Musoke A, Morzaria S, Nkonge C, Jonest E, Nene V. A recombinant sporozoite surface antigen of *Theileria parva* induces protection in cattle (East Coast fever/neutralizing antibodies/vaccine/fusion protein). Immunology. 1992;89:514–8.
Musoke A, Rowlands J, Nene V, Nyanjui J, Katende J, Spooner P, et al. Subunit vaccine based on the p67 major surface protein of *Theileria parva* sporozoites reduces severity of infection derived from field tick challenge. Vaccine. 2005;23:3084–95.
Musoke AJ, Nantulya VM, Rurangirwa FR, Busch G. Evidence for a common protective antigenic determinant on sporozoites of several *Theileria parva* strains. Immunology. 1984;30:709.
Nene V, Gobright E, Bishop R, Morzaria S, Musoke A. Linear peptide specificity of bovine antibody responses to p67 of *Theileria parva* and sequence diversity of sporozoite-neutralizing epitopes: implications for a vaccine. Infect Immun. 1999;67: 1261–6.
Nene V, Iams KP, Gobright E, Musoke AJ. Characterisation of the gene encoding a candidate vaccine antigen of *Theileria parva* sporozoites. Mol Biochem Parasitol. 1992;51:17–27.
Nene V, Morrison WI. Approaches to vaccination against *Theileria parva* and Theileria annulata. Parasite Immunol. 2016;38: 724–34.
Nene V, Musoke A, Gobright E, Morzaria S. Conservation of the sporozoite p67 vaccine antigen in cattle-derived *Theileria parva* stocks with different cross-immunity profiles. Infect Immun. 1996;64:2056–61.
Norval RAI, Perry BD, Young AS. Young AS the epidemiology of theileriosis in Africa. San Diego: Academic Press; 1992.
Nyagwange J, Nene V, Mwalimu S, Henson S, Steinaa L, Nzau B, et al. Antibodies to in silico selected GPI-anchored *Theileria parva* proteins neutralize sporozoite infection in vitro. Vet Immunol Immunopathol. 2018;199:8–14.
Painter J, Merritt EA. Optimal description of a protein structure in terms of multiple groups undergoing TLS motion. Acta Crystallogr D Biol Crystallogr. 2006;62:439–50.
Perry BD. The control of East Coast fever of cattle by live parasite vaccination: a science-to-impact narrative. One Health. 2016;2: 103–14.
Persson H, Ye W, Wernimont A, Adams JJ, Koide A, Koide S, et al. CDR-H3 diversity is not required for antigen recognition by synthetic antibodies. J Mol Biol. 2013;425:803–11.
Petitdidier E, Pagniez J, Pissarra J, Holzmuller P, Papierok G, Vincendeau P, et al. Peptide-based vaccine successfully induces protective immunity against canine visceral leishmaniasis. NPJ Vaccines. 2019;4:1–9.
Radley DE, Brown CGD, Cunningham MP, Kimber CD, Musisi FL, Payne RC, et al. East coast fever: 3. Chemoprophylactic immunization of cattle using oxytetracycline and a combination of theilerial strains. Vet Parasitol. 1975;1:51–60.
Shaw MK, Tilney LG, Musoke AJ, Teale AJ. MHC class I molecules are an essential cell surface component involved in *Theileria parva* sporozoite binding to bovine lymphocytes. J Cell Sci. 1995;108:1587–96.
Tebaldi G, Williams LB, Verna AE, Macchi F, Franceschi V, Fry LM, et al. Assessment and optimization of *Theileria parva* sporozoite full-length p67 antigen expression in mammalian cells. PLoS Negl Trop Dis. 2017;11:e0005803.
Teyra J, Huang H, Jain S, Guan X, Dong A, Liu Y, et al. Comprehensive analysis of the human SH3 domain family reveals a wide variety of non-canonical specificities. Structure. 2017;25:1598–1610.e3.
Urzhumtsev A, Afonine PV. Adams PD TLS from fundamentals to practice. Crystallogr Rev. 2013;19:230–70.
van den Ent F, Löwe J. RF cloning: a restriction-free method for inserting target genes into plasmids. J Biochem Biophys Methods. 2006;67(1):67–74. https://doi.org/10.1016/j.jbbm.2005.12.008
Wright JD, Lim C. A fast method for predicting amino acid mutations that lead to unfolding. Protein Eng. 2001;14:479–86.
Xu F, Yuan Y, Wang Y, Yin Q. Emerging peptide-based nanovaccines: from design synthesis to defense against cancer and infection. Biomed Pharmacother. 2023;158:114117.

How to cite this article: Miersch S, Singer AU, Chen C, Fellouse F, Gopalsamy A, Costa LSe, et al. Molecular characterization of a synthetic neutralizing antibody targeting p67 of *Theileria parva*. Protein Science. 2025;34(6):e70153. https://doi.org/10.1002/pro.70153